© 2016. Published by The Company of Biologists Ltd | Journal of Experimental Biology (2016) 219, 1346-1355 doi:10.1242/jeb.134494

RESEARCH ARTICLE

An animal homolog of plant Mep/Amt transporters promotes ammonia excretion by the anal papillae of the disease vector mosquito *Aedes aegypti*

Helen Chasiotis[1], Adrian Ionescu[1], Lidiya Misyura[1], Phuong Bui[1], Kimberly Fazio[2], Jason Wang[2], Marjorie Patrick[2], Dirk Weihrauch[3] and Andrew Donini[1,*]

ABSTRACT

The transcripts of three putative ammonia (NH_3/NH_4^+) transporters, Rhesus-like glycoproteins *AeRh50-1*, *AeRh50-2* and Amt/Mep-like *AeAmt1* were detected in the anal papillae of larval *Aedes aegypti*. Quantitative PCR studies revealed 12-fold higher transcript levels of *AeAmt1* in anal papillae relative to *AeRh50-1*, and levels of *AeRh50-2* were even lower. Immunoblotting revealed AeAmt1 in anal papillae as a pre-protein with putative monomeric and trimeric forms. AeAmt1 was immunolocalized to the basal side of the anal papillae epithelium where it co-localized with Na^+/K^+-ATPase. Ammonium concentration gradients were measured adjacent to anal papillae using the scanning ion-selective electrode technique (SIET) and used to calculate ammonia efflux by the anal papillae. dsRNA-mediated reductions in AeAmt1 decreased ammonia efflux at larval anal papillae and significantly increased ammonia levels in hemolymph, indicating a principal role for AeAmt1 in ammonia excretion. Pharmacological characterization of ammonia transport mechanisms in the anal papillae suggests that, in addition to AeAmt1, the ionomotive pumps V-type H^+-ATPase and Na^+/K^+-ATPase as well as NHE3 are involved in ammonia excretion at the anal papillae.

KEY WORDS: Na^+/K^+-ATPase, V-type H^+-ATPase, NHE3, Carbonic anhydrase, Ammonium transporter, Rhesus glycoprotein

INTRODUCTION

Ammonia (NH_3/NH_4^+) is a compound of major importance to life on earth, serving as an important nutrient for microorganisms and plants while presenting challenges to animals because of its toxic nature. While plants and microorganisms typically scavenge for ammonia in order to incorporate the nitrogen into proteins, animals excrete it as a toxic by-product of metabolic protein breakdown. Members of the methylammonium permease/ammonium transporter (Mep/Amt) family of transporters play a critical role in ammonia uptake by plants and microorganisms (Thornton et al., 2006; Nygaard et al., 2006; Willmann et al., 2007; Gu et al., 2013; Wu et al., 2015). The annotated genomes of vertebrate animals lack Mep/Amt homologs and excretion of ammonia in animals has been linked to members of a related family of glycoproteins, the Rhesus glycoproteins (RhGPs) (Nawata et al., 2007; Braun et al., 2009; Shih et al., 2013). Interestingly, homologs of the Mep/Amt transporters are present in the invertebrates along with homologs of RhGPs (Weihrauch et al., 2012b; Fig. 1).

In the mosquito *Aedes aegypti*, three putative ammonia transporter genes were identified *in silico* and named *AeRh50-1*, *AeRh50-2* (sharing sequence similarity with RhGPs) and *AeAmt1* (similar to Mep/Amt) (Weihrauch et al., 2012b). In a gene analysis, the *AeAmt1* gene aligns with other invertebrate Mep/Amt homologs and these are most similar to the Mep/Amt genes of plants (see Fig. 1). The *AeRh50-1* and *AeRh50-2* genes align with other RhGP homologs of insects and other invertebrates (Fig. 1). The *Aedes* RhGPs possess the conserved ammonia conducting amino acid residues that have been identified in the vertebrate RhGPs, and AeAmt1 shares 22% sequence identity with the bacterial AmtB and also contains amino acid residues in the pore that are critical to ammonia transport (Weihrauch et al., 2012b). There is ample evidence from other animals to suggest that RhGPs transport NH_3 preferentially over NH_4^+ (see Gruswitz et al., 2010; Nawata et al., 2010; Nakhoul and Hamm, 2014). Although the exact mechanism of transport by RhGPs is still up for debate, a model for NH_3 transport by human RhCG relies on comparisons with a model proposed for transport by AmtB (see below) and suggests that RhCG may recruit NH_4^+ (Gruswitz et al., 2010). The NH_4^+ is then deprotonated and NH_3 is transported and released at the other side of the membrane (Gruswitz et al., 2010). The RhGPs have also been implicated in conducting CO_2 across cellular membranes (Soupene et al., 2004; Kustu and Inwood, 2006; Peng and Huang, 2006; Perry et al., 2010). In contrast, evidence suggests that the plant and microorganism Mep/Amts transport NH_4^+ (Willmann et al., 2007; Yuan et al., 2009; Gu et al., 2013; Wu et al., 2015). The exact mechanism of transport is the subject of debate; however, one study proposes that AmtB recruits NH_4^+ and as the NH_4^+ travels further into the channel it is deprotonated yielding NH_3 (Khademi et al., 2004). The NH_3 then passes through the central hydrophobic region of the AmtB, and as it emerges it receives a proton, yielding NH_4^+, which is released to the other side of the membrane (Khademi et al., 2004). Hence, AmtB mediates net NH_4^+ transport. The Amt transporters of *Arabidopsis* have also been shown to carry out net NH_4^+ transport (see Yuan et al., 2009). To date, the only animal Mep/Amt homolog that has been studied in any detail is the mosquito AgAmt of *Anopheles gambiae* (Pitts et al., 2014). It was suggested that AgAmt transports NH_4^+ as heterologous expression of AgAmt in *Xenopus* oocytes bathed in NH_4Cl (200 nmol l^{-1} to 500 mmol l^{-1}) resulted in a positive inward current; however, the ionic nature of the current was not determined and a yeast complementation study for AgAmt failed to demonstrate ammonia transport (Pitts et al., 2014). Transcript abundance of *AgAmt* was enriched in the antennae of adult mosquitoes, leading the authors to suggest a role in sensing volatile ammonia during host-seeking behavior (Pitts et al., 2014).

[1]Department of Biology, York University, 4700 Keele Street, Toronto, Ontario, Canada M3J 1P3. [2]Department of Biology, University of San Diego, 5998 Alcala Park, San Diego, CA 92110, USA. [3]Department of Biological Sciences, University of Manitoba, 50 Sifton Road, Winnipeg, Manitoba, Canada R3T 2N2.

*Author for correspondence (adonini@yorku.ca)

Received 9 November 2015; Accepted 22 February 2016

Journal of Experimental Biology

Journal of Experimental Biology (2016) 219, 1346-1355 doi:10.1242/jeb.134494

Whereas *A. gambiae* is a major vector for malaria, *Aedes aegypti* is the vector for re-emerging tropical diseases dengue and chikungunya virus. Larval control measures traditionally focus on freshwater habitats; however, it was shown that *A. aegypti* naturally breeds in brackish water and ammonia-rich septic tanks in Asia and the Caribbean (Burke et al., 2010; Ramasamy and Surendran, 2012). In the case of the latter, it was suggested that this discovery explains the persistence of dengue during drier seasons as the mosquitoes breeding in septic tanks act as a reservoir for the disease (Burke et al., 2010). As ammonia is toxic to all animals, investigating how larval *A. aegypti* excrete ammonia is particularly important in light of their ability to breed in septic

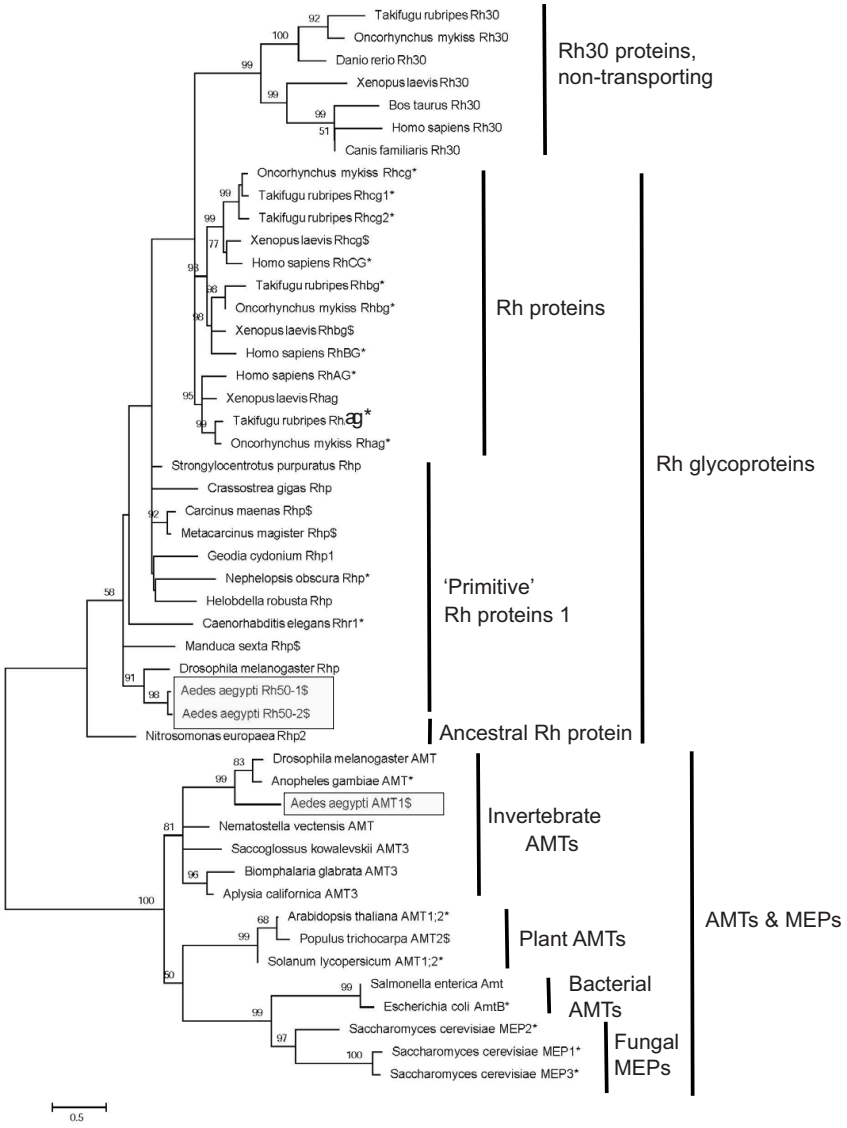

Fig. 1. Unrooted maximum likelihood tree for Rhesus (Rh) proteins, methylammonium permeases (Meps) and ammonium transporters (Amts). Numbers beside branches represent bootstrap values from 1000 replicates. The tree branches are drawn to scale, with the scale bar representing the number of amino acid substitutions per site. *Sequences with a confirmed ammonia transport capability; $sequences with suggested ammonia transport capability based on indirect evidence. The boxed sequences are the subject of the current study. Species name, gene and GenBank accession number (in parentheses): *Bos taurus* Rh30 (AAD11526.1), *Canis familiaris* Rh30 (AAX39718.1), *Danio rerio* Rh30 (AAU81655.1), *Homo sapiens* Rh30 (CAA38401.1), *Oncorhynchus mykiss* Rh30 (AAP87367.1), *Takifugu rubripes* Rh30 (AAM48580.2), *Xenopus laevis* Rh30 (AAR00222.1), *Homo sapiens* RhAG (AAC04247.1), *Oncorhynchus mykiss* Rhag (ABV24962.1), *Takifugu rubripes* Rhag (AAV28817.1), *Xenopus laevis* Rhag (BAB13345.1), *Homo sapiens* RhBG (AAG01086.1), *Oncorhynchus mykiss* Rhbg-1 (ABO16485.1), *Takifugu rubripes* Rhbg (AAM48577.1), *Xenopus laevis* Rhbg (AAR08675.1), *Homo sapiens* RhCG (AAF19372.1), *Oncorhynchus mykiss* Rhcg (AAU89494.1), *Takifugu rubripes* Rhcg1 (AAM48578.1), *Takifugu rubripes* Rhcg2 (AAM48579.1), *Xenopus laevis* Rhcg (AAH84943.1), *Aedes aegypti* Rh50-1 (AY926463.1), *Aedes aegypti* Rh50-2 (AY926464.1), *Caenorhabditis elegans* Rhr-1 (AAF97864.1), *Carcinus maenas* Rhp (AAK50057.2), *Crassostrea gigas* Rhp (EKC21768.1), *Drosophila melanogaster* Rhp (AF193812), *Geodia cydonium* Rhp1 (CAA73029.1), *Helobdella robusta* Rhp (XP_009016010.1), *Manduca sexta* Rhp (ABI20766.1), *Metacarcinus magister* Rhp (AEA41159.1), *Nephelopsis obscura* Rhp (KM923907), *Strongylocentrotus purpuratus* Rhp (XP_789738.3), *Nitrosomonas europaea* Rhp2 (AAR24581.1), *Aedes aegypti* Amt1 (DQ011229), *Anopheles gambiae* AMT (XM_318439), *Aplysia californica* AMT3 (XP_012946834.1), *Biomphalaria glabrata* AMT3 (XP_013085164.1), *Drosophila melanogaster* AMT (NP_001097800), *Nematostella vectensis* AMT (XP_001639101.1), *Saccoglossus kowalevskii* AMT3 (XP_006819255.1), *Arabidopsis thaliana* AMT 1;2 (NP_176658.1), *Populus trichocarpa* AMT2 (XP_002325790.2), *Solanum lycopersicum* AMT1;2 (O04161.1), *Escherichia coli AmtB* (1U77_A), *Salmonella enterica* Amt (WP_049281994.1), *Saccharomyces cerevisiae* MEP1 (NP_011636), *Saccharomyces cerevisiae* MEP2 (CAA96025), *Saccharomyces cerevisiae* MEP3 (EGA76487).

Journal of Experimental Biology

Journal of Experimental Biology (2016) 219, 1346-1355 doi:10.1242/jeb.134494

tanks. Other aquatic freshwater animals exploit the habitat and excrete ammonia directly into the water without the costly conversion to less-toxic forms (García Romeu and Salibián, 1968; Weihrauch et al., 2004; Nawata et al., 2007; Weihrauch et al., 2012a, b; Cruz et al., 2013). Through work on frog skin, planarians, and crustacean and fish gills, a number of cellular mechanisms and transporters for ammonia excretion in freshwater animals have been discovered. In addition to the RhGPs and the Mep/Amts, these include members of the solute carrier family 9 (SLC9, NHEs) (Orlowski and Grinstein, 2004; Zachos et al., 2005); the Na^+/K^+-ATPase (NKA) (Masui et al., 2002; Furriel et al., 2004; Weihrauch et al., 2012b; Ip et al., 2012); and the V-type H^+-ATPase (VA) (Wilson et al., 1994; Shih et al., 2008; Braun et al., 2009; Weihrauch et al., 2009; Wright and Wood, 2009).

In general, the excretory organs of insects include the Malpighian tubules and hindgut; however, larvae of *A. aegypti* also possess four anal papillae that are finger-like structures surrounding the anus and composed of a simple, syncytial epithelium covered by a thin cuticle with a luminal space that is continuous with the hemocoel of the body (Edwards and Harrison, 1983). A previous study detected ammonia effluxes (excretion) by the anal papillae using the scanning ion-selective electrode technique (SIET) (Donini and O'Donnell, 2005). It was determined that the anal papillae of larval mosquitoes excrete ammonia at a rate of 360 nmol cm^{-2} h^{-1}, which is consistent with rates of ammonia excretion by the locust hindgut and by the cockroach *Periplaneta americana* (Mullins, 1974; Thomson et al., 1988; Donini and O'Donnell, 2005). Therefore, the anal papillae appear to be major sites of ammonia excretion in larval mosquitoes.

The aim of this study was to elucidate the epithelial transport mechanisms of ammonia excretion by the anal papillae of *A. aegypti*. We hypothesized that the anal papillae express the putative ammonia transporters and that these transporters are involved in the observed ammonia excretion from the anal papillae. To test this hypothesis, the study examined the transcript abundance of the three putative *Aedes* ammonia transporters in the anal papillae and pursued further studies on the putative transporter that showed enriched transcript abundance (*AeAmt1*).

MATERIALS AND METHODS

Phylogenetic analysis of Rhesus glycoproteins, Meps and Amts

The amino acid sequences were aligned by MUSCLE alignment in MEGA 5. Gene analysis of the aligned sequences was also performed with MEGA 5 using the maximum likelihood method with the Jones–Taylor–Thornton+four categories of gamma substitution rates+invariable sites model and nearest-neighbor interchange (NNI) heuristic method. Bootstrap values were determined from 1000 bootstrap replicates.

Animals

Larvae of *A. aegypti* (Liverpool) were obtained from a colony reared in the Department of Biology, York University (Toronto, ON, Canada). Larvae were reared in reverse-osmosis (RO) water at room temperature and on a 12 h:12 h light:dark cycle. Larvae were fed daily with a solution of liver powder and yeast in water. Rearing water was refreshed every other day. Fourth instar larvae were used 24 h post-feeding for all pharmacological studies. For molecular experiments, the larvae were fasted for 72 h prior to use.

Reverse transcription-PCR and quantitative PCR

Seven biological samples, each consisting of a pool of 200 anal papillae from 50 larvae, were isolated in cold *A. aegypti* physiological saline (Clark and Bradley, 1996) prepared in diethylpyrocarbonate (DEPC; Sigma-Aldrich, Oakville, ON, Canada) treated water. Harvested tissues were transferred to tubes containing TRIzol® RNA isolation reagent (Invitrogen, Burlington, ON, Canada) and sonicated for 5 s at 5 W using an XL 2000 Ultrasonic Processor (Qsonica, LL, CT, USA). RNA was extracted according to TRIzol® specifications and treated with the TURBO DNA-free™ Kit (Applied Biosystems, Streetsville, ON, Canada) to remove genomic DNA. RNA samples were used to synthesize cDNA using the iScript™ cDNA Synthesis Kit (Bio-Rad, Mississauga, ON, Canada) according to the manufacturer's instructions. The cDNA was stored at −20°C until subsequent use. Genes encoding putative *A. aegypti* ammonia transporters (*AeRh50-1*, *AeRh50-2* and *AeAmt1*) were found in the *A. aegypti* genome in the National Center for Biotechnology Information (NCBI) database (http://www.ncbi.nlm.nih.gov) and the sequences used to design primers. Primer sequences, amplicon sizes and related accession numbers are listed in Table 1. Reverse transcription polymerase chain reaction (RT-PCR) was used to check for the presence of transcripts of putative ammonia transporters in *A. aegypti* anal papillae with *18S rRNA* serving as an internal control. Amplicons were resolved by gel electrophoresis and sequenced at the York University sequencing facility (York University Core Molecular Facility, Toronto, ON, Canada). Sequence identities were confirmed by a BLAST search (NCBI database; http://www.ncbi.nlm.nih.gov).

To determine the relative mRNA abundance of *AeRh50-1*, *AeRh50-2* and *AeAmt1* in larval *A. aegypti* anal papillae, quantitative PCR (qPCR) was performed using the primers listed in Table 1 and SsoFast™ Evagreen® Supermix (Bio-Rad) according to the manufacturer's protocol. Reactions were carried out using the CFX96™ real-time PCR detection system (Bio-Rad). To confirm the presence of a single product after each reaction, a melting curve analysis was performed. For each gene of interest, a standard curve was generated to optimize reaction efficiency. Quantification of transcripts was determined according to the Pfaffl method (Pfaffl, 2004). Samples were run in duplicate and *18S rRNA* was used as an internal control because it showed consistent levels of expression under experimental treatments. A no-template negative control was also used.

Western blotting and immunohistochemistry

Western blotting and immunohistochemistry for AeAmt1 and NHE3 were carried out at York University and the University of San Diego (CA, USA), respectively. Biological samples consisting of pools of 10–15 *A. aegypti* larval whole bodies or pools of anal

Table 1. Primer information for RT-PCR and qRT-PCR studies

Gene	Accession no.	Forward primer 5′–3′	Reverse primer 5′–3′	Amplicon size (bp)	Annealing temp. (°C)
AeRh50-1	AY926463.1	AAAATGCAACCGTTCCGC	GAATCCGAAACCGATGAAGA	110	60
AeRh50-2	AY926464.1	CCACATTGACCGAAGAGGA	TTGCTCCAGTTGACGCATAG	176	60
AeAMT1	DQ011229.1	GAGCATGAAGCTGATGGAC	GTATCCTCCTCCCATGAGC	180	57
18S	U65375.1	TTGATTCTTGCCGGTACGTG	TATGCAGTTGGGTAGCACCA	194	58

Journal of Experimental Biology

Journal of Experimental Biology (2016) 219, 1346-1355 doi:10.1242/jeb.134494

papillae that were isolated from 25–50 larvae under ice-cold saline were collected and stored at −80°C until later processing. For examination of AeAmt1 expression, samples were thawed on ice and larval whole bodies were sonicated in a homogenization buffer containing 50 mmol l^{-1} Tris-HCl pH 7.4, 1 mmol l^{-1} PMSF and 1:200 protease inhibitor cocktail (Sigma-Aldrich), while anal papillae were sonicated in a homogenization buffer containing 50 mmol l^{-1} Tris-HCl pH 7.5, 150 mmol l^{-1} NaCl, 1% sodium deoxycholate, 1% Triton X-100, 0.1% SDS, 1 mmol l^{-1} PMSF and 1:200 protease inhibitor cocktail (Sigma-Aldrich). All samples were sonicated for 2×10 s at 3.5 W using an XL 2000 Ultrasonic Processor (Qsonica). For NHE3 expression, 80 µl of homogenization buffer (as described above) was added to a 1.5 ml centrifuge tube containing anal papillae tissue and then homogenized on ice for 30 s using a hand-held tissue grinder (Kontes Pellet Pestle). Homogenates were then centrifuged at 8000 or 10,000 ***g*** for 8 or 10 min at 4°C, and the protein content of the collected supernatants was determined using the Bradford assay (Sigma-Aldrich or Bio-Rad) according to the manufacturer's guidelines. Whole-body samples and anal papillae samples for NHE3 expression were prepared for SDS-PAGE by heating for 10 min at 95°C in 5× loading buffer containing 225 mmol l^{-1} Tris-HCl pH 6.8, 3.5% (w/v) SDS, 35% glycerol, 12.5% (v/v) β-mercaptoethanol and 0.01% (w/v) Bromophenol Blue, while anal papillae samples for AeAmt1 expression were prepared by heating for 5 min at 100°C in 6× loading buffer containing 360 mmol l^{-1} Tris-HCl pH 6.8, 12% (w/v) SDS, 30% glycerol, 600 mmol l^{-1} DTT and 0.03% (w/v) Bromophenol Blue. Samples (5–7 µg protein) were then electrophoretically separated by SDS-PAGE and western blot analysis of AeAmt1 was conducted according to a previously described protocol (Chasiotis and Kelly, 2008), while analysis of NHE3 was carried out by overnight transfer of protein to Immobilon-P polyvinylidene-difluoride (PVDF) membrane (EMD Millipore, USA) at 4°C. A custom-made polyclonal antibody that was produced in rabbit against a custom-made synthetic peptide (CPLWEREVELSDGLM) corresponding to a 14-amino acid region of AeAmt1 (GenScript USA Inc., Piscataway, NJ, USA) was used at 1:500 dilution. To confirm the specificity of the custom-made AeAmt1 antibody, a comparison blot was also run with the AeAmt1 antibody pre-absorbed with 10× molar excess of the immunogenic peptide for 1 h at room temperature prior to application to blots. After examination of AeAmt1 expression, blots were stripped and re-probed with a 1:100 dilution of mouse monoclonal anti-JLA20 antibody (J. J.-C. Lin, Developmental Studies Hybridoma Bank, Iowa City, IA, USA) for actin or a 1:1000 dilution of rabbit monoclonal anti-GAPDH (14C10) antibody (New England BioLabs, Whitby, ON, Canada) as loading controls. Densitometric analysis of AeAmt1, actin and GAPDH was conducted using Quantity One 1D analysis software (Bio-Rad). AeAmt1 abundance was expressed as a normalized value relative to the abundance of the loading control. Detection of NHE3 was performed using Life Technologies Western Breeze anti-rabbit chemiluminescent kit and an antibody generated against the C-terminal residues (E^{1111}-G^{1128}) of *A. aegypti* NHE3 (Pullikuth et al., 2006) diluted to 1:5000. Detection of protein bands were performed using Bio-Rad ChemiDoc XRS system.

Immunolocalization of AeAmt1, NKA, VA and NHE3 in paraffin-embedded sections of anal papillae was conducted according to previously described protocols (Pullikuth et al., 2006; Chasiotis and Kelly, 2008) using a 1:40 dilution of the custom-made anti-AeAmt1 antibody described above, a 1:10 dilution of a mouse monoclonal anti-α5 antibody for NKA (Douglas Fambrough, Developmental Studies Hybridoma Bank, IA, USA), a 1:100 dilution of a mouse polyclonal anti-ATP6V0A1 antibody for VA (Abnova, Taipei, Taiwan) or a 1:250 dilution of the NHE3 antibody described above. A sheep anti-mouse antibody conjugated to Cy2 or a goat anti-mouse antibody conjugated to Cy5 (Jackson Immunoresearch) was applied at 1:500 and 1:1000, respectively, to visualize NKA. The same sheep anti-mouse antisera applied at 1:500 was used to visualize VA. A goat anti-rabbit antibody conjugated to Alexa Fluor 594 (Jackson Immunoresearch) was applied at 1:500 dilution to visualize AeAmt1, while a goat anti-rabbit antibody conjugated to Alexa Fluor 647 (Jackson Immunoresearch) was applied at 1:1000 dilution to visualize NHE3. Comparison negative control slides were also processed as described above with either all primary antibodies omitted or the AeAmt1 antibody pre-absorbed with 10× molar excess of the immunogenic peptide for 30 min at room temperature prior to application to sections. Slides were mounted using ProLong Gold antifade reagent with or without DAPI (Life Technologies, Burlington, ON, Canada), and fluorescence images were captured using either an Olympus IX71 inverted fluorescence microscope (Olympus Canada, Richmond Hill, ON, Canada) and CellSense® 1.12 Digital Imaging software (Olympus Canada) or a Nikon A1R laser scanning confocal microscope. Images were merged using Adobe Photoshop CS6 software (Adobe Systems Inc., Ottawa, ON, Canada).

dsRNA preparation and delivery, larval mortality and hemolymph NH_4^+ levels

Total RNA was extracted from whole bodies of fourth instar *A. aegypti* larvae and cDNA was generated as described above. Using this cDNA template, a fragment of the *AeAmt1* gene (849 bp) was amplified by RT-PCR using primers (forward 5′ T-TTCGTCATCTTCCACAACC 3′; reverse 5′ TCAATACCCACA-GCAAGGTC 3′) designed based on GenBank Accession no. DQ011229. A fragment of *β-lactamase* (*βLac*; 799 bp) was also amplified by RT-PCR from a pGEM-T-Easy vector (kind gift from J. P. Paluzzi, York University) using the following primers: forward 5′ ATTTCCGTGTCGCCCTTATTC 3′; reverse 5′ CGTTCATCC-ATAGTTGCCTGAC 3′. PCR products were concentrated and purified using a QIAquick PCR Purification kit (Qiagen Inc., Toronto, ON, Canada) and used to generate double stranded (ds) RNAs by *in vitro* transcription using the Promega T7 RiboMAX Express RNAi Kit (Promega, WI, USA). *AeAmt1* or *βLac* dsRNA were delivered to larvae according to a previously described protocol (Singh et al., 2013). Briefly, groups of 50 larvae (1st and 2nd instar), which were initially reared as described above, were soaked for 2 h in 75 µl PCR-grade water containing 0.5 µg $µl^{-1}$ dsRNA and then transferred into 20 ml RO water. Ingestion of the dsRNA solution by larvae was confirmed in preliminary studies by soaking larvae in a solution containing 0.5% Bromophenol Blue and then assessing accumulation of the dye in the larval gut as described previously (Singh et al., 2013). Rearing water was refreshed every 2 days following dsRNA treatment. To confirm reductions in *AeAmt1* transcript as a result of dsRNA treatment, total RNA was extracted and cDNA was generated (as described above) from pools of 10–15 larval whole bodies at days 3 and 6 post-dsRNA treatment. cDNA templates were then used in RT-PCR with the above primers and PCR products were resolved electrophoretically in a 1% agarose gel stained with ethidium bromide. Reductions in AeAmt1 in larval whole bodies and anal papillae as a result of dsRNA treatment were examined by western blotting as described above. Larval mortality between day 3 and day

Journal of Experimental Biology (2016) 219, 1346-1355 doi:10.1242/jeb.134494

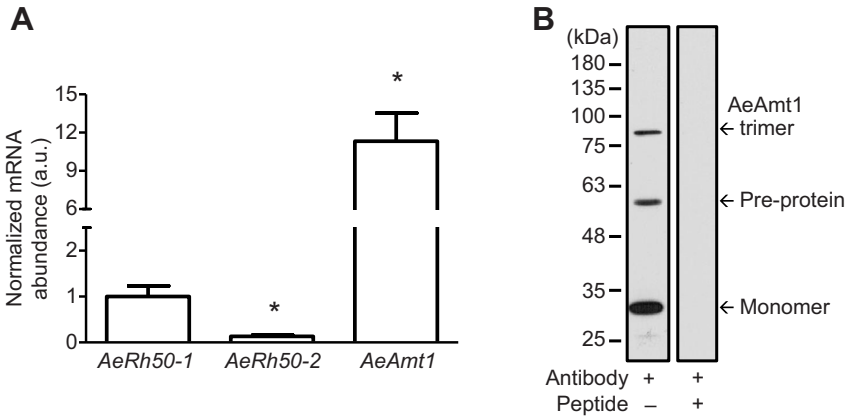

Fig. 2. Transcript expression of putative ammonia transporters and protein expression of the putative ammonia transporter AeAmt1 in anal papillae of *Aedes aegypti*. (A) Relative transcript abundance of *AeRh50-1*, *AeRh50-2* and *AeAmt1* in anal papillae of larval *A. aegypti* by qPCR. *AeRh50-1*, *AeRh50-2* and *AeAmt1* transcript abundance was normalized to *18S rRNA* and expressed relative to *AeRh50-1* transcript abundance. Data are means+s.e.m., *N*=4 for *AeAmt1* and *N*=5 for *AeRh50-1 and AeRh50-2* (a.u., arbitrary units). *Significant difference ($P<0.05$, two-tailed Student's *t*-test) from *AeRh50-1* mRNA. (B) Representative western blot of AeAmt1 in anal papillae of larval *A. aegypti* reveals an AeAmt1 pre-protein at ~55 kDa and potential monomer and trimer forms. All bands were blocked by antibody pre-absorption with the immunogenic peptide.

6 post-dsRNA treatment was determined by subtracting the number of surviving larvae on day 6 from the number of larvae counted on day 3. NH_4^+ flux across anal papillae of *A. aegypti* larvae was determined at 6 days post-dsRNA treatment by SIET (see below). The [NH_4^+] in hemolymph was measured using ion-selective microelectrodes as previously described (Jonusaite et al., 2011). Microelectrodes were backfilled with 100 mmol l^{-1} NH_4Cl and front filled with NH_4^+ ionophore I, cocktail A. Microelectrodes were calibrated in solutions of 0.1, 1 and 10 mmol l^{-1} NH_4Cl.

SIET technique

The SIET system used in this study has been described previously (Donini and O'Donnell, 2005; Nguyen and Donini, 2010). Microelectrodes were backfilled with 100 mmol l^{-1} NH_4Cl and front filled with NH_4^+ ionophore I, cocktail A (Sigma-Aldrich). Microelectrodes were calibrated in solutions of 0.1, 1 and 10 mmol l^{-1} NH_4Cl. Larvae were blotted dry on a piece of filter paper and then immobilized in a Petri dish using beeswax, such that one side of an anal papilla was exposed for measurements. Voltage gradients adjacent to the anal papilla were recorded under 4 ml of 0.5 mmol l^{-1} NH_4Cl.

The recording protocol was as follows: the ion-selective microelectrode was moved to a target site ~5 µm away from the surface of the anal papilla and a voltage was recorded. A second voltage recording was then obtained at ~105 µm from the surface of the anal papilla. The protocol was repeated four times at each target site and consisted of 4 s wait time and 1 s sampling time. Readings were taken at the middle one-third portion of the anal papilla at four target sites separated by 25–30 µm. A voltage gradient was calculated by Automated Scanning Electrode Technique software (ASET; Science Wares, East Falmouth, MA, USA), using the differences between voltage readings at the two points of each site, and is reported as the average of the four readings at each site. Background voltage readings were taken by moving the microelectrodes 2500 µm away from the preparation and employing the same sampling protocols. Background voltage gradients (noise) were then subtracted from the gradients reported at each target site.

The voltage gradients obtained from the ASET software program were converted into concentration gradients using the equation:

$$\Delta C = C_B \times 10(\Delta V/S) - C_B,$$

where ΔC is the concentration gradient (µmol l^{-1} cm^{-3}) between the two points measured at the anal papilla, C_B is the background concentration (µmol l^{-1}) of NH_4^+, ΔV is the voltage gradient (µV) obtained from the ASET software and S is the Nernst slope of the electrode. The concentration gradient was then converted into ion flux using Fick's law of diffusion:

$$J = D(\Delta C)/\Delta X,$$

where J is the net flux of the ion (pmol cm^{-2} s^{-1}), D is the diffusion coefficient (2.09×10^{-5} cm^2 s^{-1}), ΔC is the concentration gradient (pmol cm^{-3}) and ΔX is the distance between the two points measured (cm).

The NH_4^+ fluxes were recorded from larvae treated with *AeAmt1* or *βLac* dsRNA and larvae treated with pharmacological transport inhibitors in a bathing solution of 0.5 mmol l^{-1} NH_4Cl. For the latter, larvae reared in RO water were pre-incubated for 30 min under control or experimental conditions. Pre-incubated experimental larvae were exposed to the following concentration of inhibitor (transporter/mechanism targeted is given in parentheses): 100 µmol l^{-1} bafilomycin (VA); 100 µmol l^{-1}

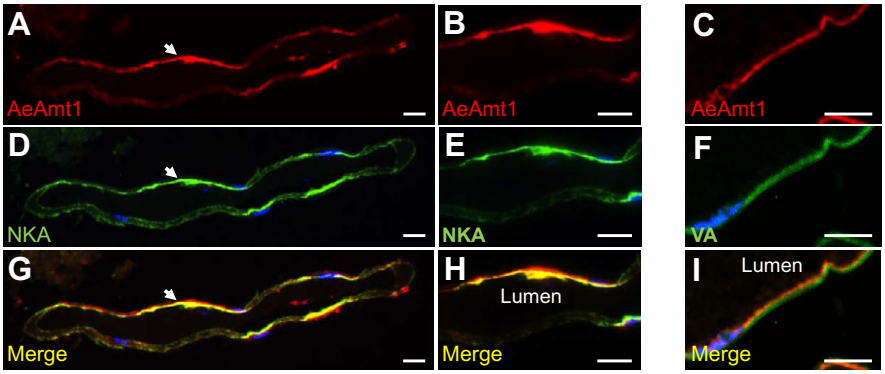

Fig. 3. Immunolocalization of AeAmt1 in anal papillae of larval *A. aegypti*. Representative paraffin-embedded sections of larval anal papillae that show immunoreactivity for: (A–C) AeAmt1 (red), (D,E) Na^+/K^+-ATPase (NKA; green) or (F) V_0 subunit of V-type H^+-ATPase (VA; green). In D–F, nuclei were also stained with DAPI (blue). (G–I) Merged images of A and D, B and E, and C and F, respectively. B, E and H show areas indicated by the white arrows in A, D and G, respectively, at a higher magnification. Scale bars, 20 µm.

Journal of Experimental Biology (2016) 219, 1346-1355 doi:10.1242/jeb.134494

ouabain (NKA); 100 µmol l^{-1} 5-(*N*,*N*)-hexamethylene amiloride, HMA (NHE); 5 µmol l^{-1} S3226 (NHE3); 100 µmol l^{-1} methazolamide (carbonic anhydrase, CA). Selection of the concentration for each inhibitor was based on previous invertebrate or vertebrate tissue studies (MacVicker et al., 1993; Marcaggi et al., 1999; Vallon et al., 2000; Weihrauch, 2006; Tsui et al., 2009; Nguyen and Donini, 2010; Del Duca et al., 2011). All the inhibitors contained 0.1% DMSO in 0.5 mmol l^{-1} NH_4Cl, therefore control larvae were pre-incubated in 0.5 mmol l^{-1} NH_4Cl containing 0.1% DMSO. The Nernst slopes of NH_4^+ ion-selective microelectrodes were (mean±s.e.m.) 51.6±0.5, *N*=6, for the dsRNA experiments and 54.3±0.5, *N*=54, for the pharmacology experiments.

Statistics

Data were analyzed using Prism® 5.03 (GraphPad Software Inc., La Jolla, CA, USA) and expressed as means±s.e.m. Two-tailed *t*-tests were used to determine significance between control and experimental groups. Control groups as well as ion-selective microelectrode calibration data were compared using a one-way ANOVA to determine statistical similarity. For SIET data, a single biological replicate is defined as the average flux of 6 sites along a single papilla from a single larva.

RESULTS

AeAmt1 expression and dsRNA knockdown in anal papillae

Quantitative analysis of transcript abundance of three putative ammonia transporters in anal papillae revealed that *AeRh50-1* transcript levels were 10-fold greater than *AeRh50-2* transcript levels (Fig. 2A). Furthermore, *AeAmt1* transcript abundance was 12- and 120-times greater than that of *AeRh50-1* and *AeRh50-2*, respectively. Western blot analysis of anal papillae from larvae revealed an AeAmt1 pre-protein, based on its putative amino acid sequence, at ∼55 kDa, and potential AeAmt1 monomer and trimer forms, which were all blocked by antibody pre-absorption with the immunogenic peptide (Fig. 2B). While the AeAmt1 monomer was always detected in western blots, the pre-protein and trimer forms were not consistently detected between samples; therefore, only the monomer form could be quantified for dsRNA-treatment experiments (see below).

AeAmt1 co-immunolocalized with basally expressed NKA in the anal papillae epithelium (Fig. 3A,D,G). However, AeAmt1 immunoreactivity was also observed in a few regions of the epithelium where NKA was not present (Fig. 3B,E,H). Although there was overlap in immunoreactivity between AeAmt1 and the V_0 subunit of VA at the interface between the apical and basal domains of the anal papillae epithelium, AeAmt1 did not co-immunolocalize

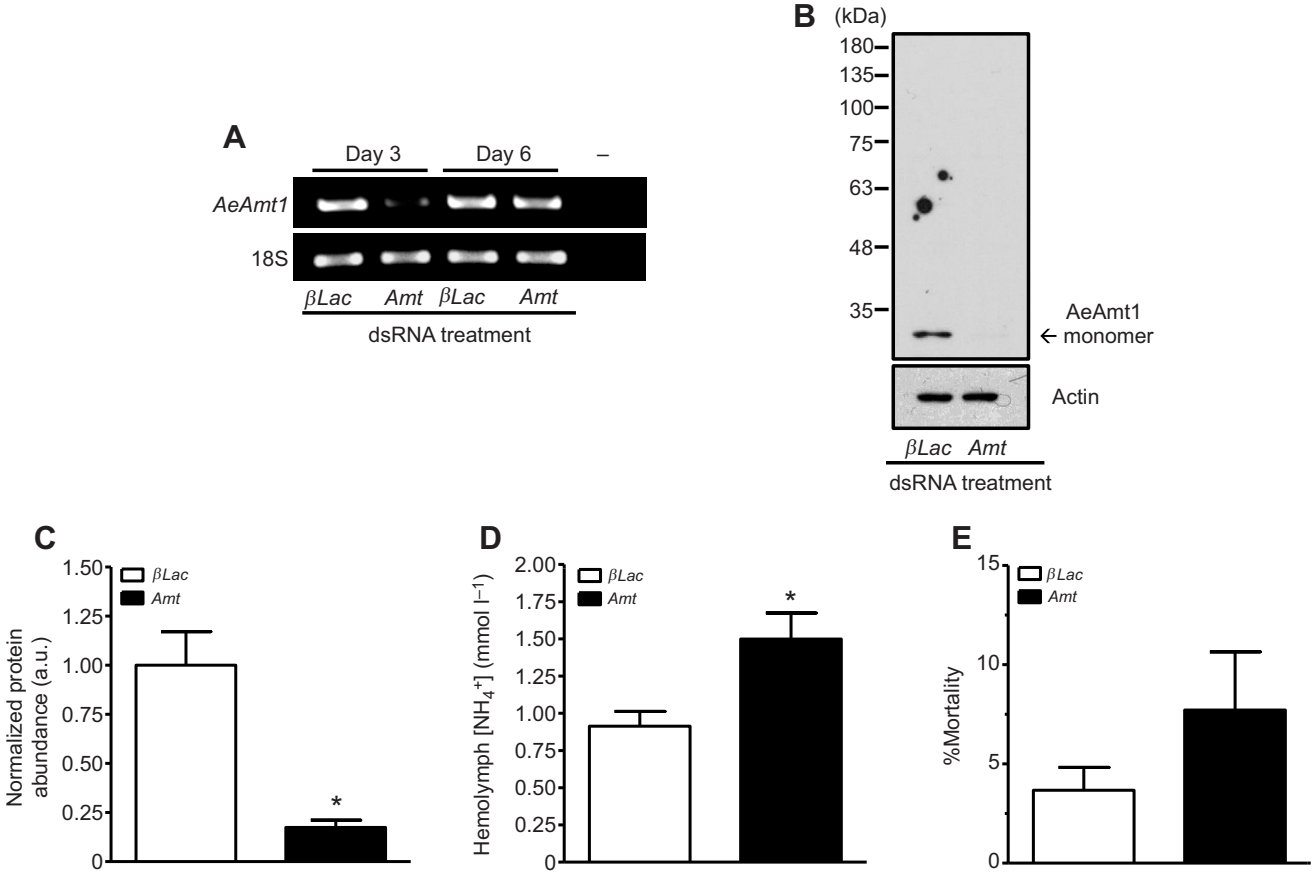

Fig. 4. Effects of *AeAmt1* dsRNA treatment on whole-body *AeAmt1* transcript and protein abundance, hemolymph NH_4^+ levels and mortality of larval *A. aegypti*. (A) Qualitative *AeAmt1* transcript expression by RT-PCR and agarose gel electrophoresis in larval whole bodies at days 3 and 6 following treatment with control *β-lactamase (βLac)* or *AeAmt1* (*Amt*) dsRNA. Negative (–) controls were prepared with no cDNA template. *18SrRNA* expression is also shown as a loading control. (B) Representative western blot and (C) densitometric analysis of AeAmt1 monomer in larval whole bodies at 6 days post-treatment with *βLac* or *AeAmt1* dsRNA. AeAmt1 monomer abundance was normalized to actin and expressed relative to the control *βLac* group (*N*=5). (D) Ion-selective microelectrode measurements of NH_4^+ in larval hemolymph at 6 days post-*βLac* or -*AeAmt1* dsRNA treatment (*N*=51 for *AeAmt1* and *N*=52 for *βLac*). (E) Larval mortality between day 3 and day 6 following treatment with *βLac* or *AeAmt1* dsRNA (*N*=6 groups of larvae). Data are expressed as means+s.e.m. *Significant difference ($P<0.05$, two-tailed Student's *t*-test) from control *βLac* group.

Journal of Experimental Biology

Journal of Experimental Biology (2016) 219, 1346-1355 doi:10.1242/jeb.134494

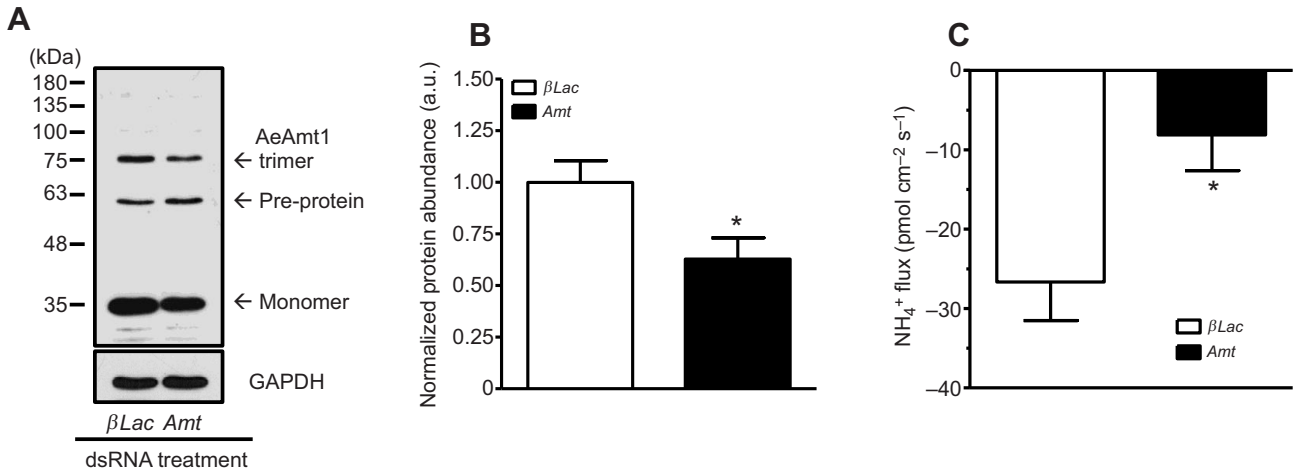

Fig. 5. Effects of *AeAmt1* dsRNA treatment on AeAmt1 abundance and NH_4^+ flux across anal papillae of larval *A. aegypti*. (A) Representative western blot and (B) densitometric analysis of AeAmt1 monomer in larval anal papillae (*N*=4), and (C) measurements of NH_4^+ flux across larval anal papillae by scanning ion-selective electrode technique (SIET) (*N*=32 for *βLac* and *N*=39 for *AeAmt1*) at 6 days following treatment with control *βLac* or *AeAmt1* dsRNA. AeAmt1 monomer abundance was normalized to GAPDH and expressed relative to the *βLac* group. Data are expressed as means±s.e.m. *Significant difference (*P*<0.05, two-tailed Student's *t*-test) from *βLac* group.

with the apically expressed V_0 subunit (Fig. 3C,F,I). Immunostaining was absent in control sections that were probed with secondary antibodies only or with AeAmt1 antibody that was pre-absorbed with the immunogenic peptide (not shown).

Larvae treated with *AeAmt1* dsRNA showed a qualitative reduction in AeAmt1 transcript at day 3 post-*AeAmt1* dsRNA treatment (Fig. 4A), and while there was an apparent recovery of transcript levels at day 6 post-treatment, the protein monomer was significantly reduced (Fig. 4B,C). Also, at day 6 post-treatment with *AeAmt1* dsRNA, larvae had elevated NH_4^+ levels in hemolymph (Fig. 4D); however, although there was an apparent increase in larval mortality, this was not statistically significant (Fig. 4E). Anal papillae of larvae at day 6 post-*AeAmt1* dsRNA treatment showed a ~37% reduction in AeAmt1 monomer levels when compared with *βLac* dsRNA-treated groups (Fig. 5A,B). NH_4^+ flux measurements across the anal papillae of larvae by SIET at day 6 post-*AeAmt1* dsRNA treatment also showed a ~3.3-fold decrease relative to control animals (Fig. 5C).

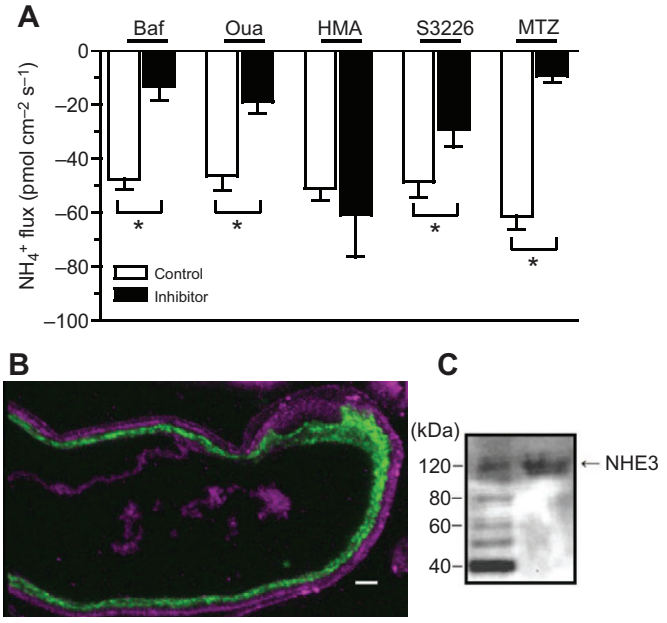

Fig. 6. Effects of transport inhibitors on NH_4^+ efflux and protein expression of NHE3 at the anal papillae of larval *A. aegypti*. (A) NH_4^+ flux measurements were conducted by SIET with an individual separate control group of larvae for each inhibitor tested: bafilomycin (Baf, *N*=10), ouabain (Oua, *N*=11), 5-(*N*,*N*)-hexamethylene amiloride (HMA, *N*=11), S3226 (*N*=10) and methazolamide (MTZ, *N*=10). Data are expressed as means+s.e.m. *Significant difference (*P*<0.05, two-tailed Student's *t*-test) from individual control group. (B) Immunolocalization of NHE3 (violet) and NKA (green) to the apical and basal side of the anal papillae epithelium, respectively. Scale bar, 10 µm. (C) Western blot analysis of NHE3 with molecular mass standards (left lane) and anal papillae homogenate (right lane) revealing a band of ~120 kDa.

Pharmacological transport inhibitors and ammonium fluxes

Incubation of larvae in the VA inhibitor bafilomycin A1 resulted in a reduction of net ammonia efflux (measured as $[NH_4^+]$ gradient) at the anal papillae from 47.6 to 13.3 pmol cm^{-2} s^{-1} (Fig. 6A). A similar result was obtained with ouabain, an inhibitor of NKA, which resulted in net NH_4^+ fluxes that were less than half of flux rates measured at the papillae of control larvae (Fig. 6A). In contrast, the NHE inhibitor HMA did not alter the NH_4^+ fluxes at the anal papillae (Fig. 6A); however, the specific NHE3 inhibitor S3226 decreased NH_4^+ efflux (Fig. 6A). NHE3 was localized to the apical side of the anal papilla epithelium (Fig. 6B) and western blots of anal papillae homogenate revealed a 120 kDa band corresponding to the predicted size of the high molecular mass variant of *A. aegypti* NHE3 (Fig. 6C). The CA inhibitor methazolamide resulted in NH_4^+ fluxes that were only 15% of flux rates recorded at papillae of control larvae (Fig. 6A).

DISCUSSION

Putative ammonia transporters in the anal papillae of the larval mosquito

The transcripts of three putative ammonia transporters *AeRh50-1*, *AeRh50-2* and *AeAmt1* were detected in the anal papillae of *A. aegypti* larvae in agreement with our hypothesis (Weihrauch et al., 2012b; Fig. 2A). The transcript abundance of *AeAmt1* was significantly greater than that of the RhGP homologs (Fig. 2A). In light of this and the previously recorded ammonia efflux at the anal papillae, we focused our work on the *Aedes* Mep/Amt homolog. NKA and VA have been localized to the basal and apical

Journal of Experimental Biology (2016) 219, 1346-1355 doi:10.1242/jeb.134494

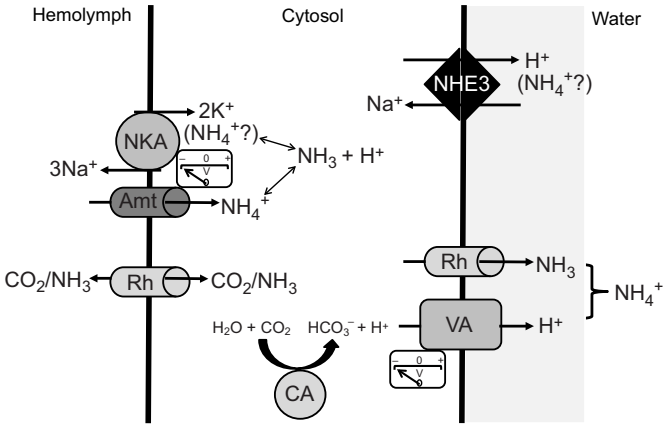

Fig. 7. Model of putative transcellular NH_3/NH_4^+ transport mechanisms in the anal papilla syncytial epithelium of the larval *A. aegypti* mosquito. On the basal side, NKA provides a cytosol negative voltage potential that could serve to drive NH_4^+ from the hemolymph to the cytosol through AeAmt1 (Amt). NH_4^+ may also enter directly through NKA by substituting for K^+. In addition, CO_2 and NH_3 may enter the cytosol through one of the two Rhesus glycoprotein (RhGP)-like proteins AeRh50-1 and/or AeRh50-2 (Rh). NH_4^+ in the cytosol may exit from the apical side to the aqueous habitat through NHE3 in exchange for a cation (e.g. Na^+). NH_3 in the cytosol may exit the apical side via one of the two RhGP-like proteins (Rh) with the aid of an ammonia-trapping mechanism whereby apical VA acidifies the papilla boundary layer. NHE3 may also participate in this mechanism by moving H^+ into the water. This would sustain the outward-directed NH_3 gradient by converting NH_3 to NH_4^+. A cytoplasmic carbonic anhydrase (CA) can supply H^+ to the VA and is also likely participating in generating the cytosol negative potential that drives NH_4^+ into the cytosol on the basal side.

membranes of the anal papillae epithelium, respectively (Patrick et al., 2006), and were therefore used to delineate the localization of AeAmt1 in larval anal papillae. Co-immunolocalization of AeAmt1 with NKA (Fig. 3G) indicates expression of AeAmt1 on the basal side. In freshwater-reared *A. aegypti* larvae, the basal membrane of the anal papillae epithelium forms extensive and deep folds into the cytoplasm that can extend more than halfway into each epithelial cell (Sohal and Copeland, 1966). Given that AeAmt1 did not co-immunolocalize with VA, but some overlap at the interface between AeAmt1 and VA was observed (Fig. 3I), it is likely that AeAmt1 expression extends into the deep infoldings of the basal membrane of the anal papillae epithelium where NKA is not present (Fig. 3H).

dsRNA-mediated reductions of AeAmt1 in larval *A. aegypti* (Figs 4 and 5) were associated with significantly decreased NH_4^+ efflux from anal papillae (Fig. 5C) and elevated levels of NH_4^+ in larval hemolymph (Fig. 4D). In larvae of freshwater zebrafish, an Rh50 protein, Rhcg1, is required along with VA to actively excrete ammonia against a higher external concentration (Shih et al., 2013). The transcript abundance of *Rhcg1* and VA increases with exposure to high environmental ammonia (HEA) and the capacity for ammonia excretion by ammonia-excreting cells increases (Braun et al., 2009). HEA exposure of the fully aquatic, freshwater-inhabiting African clawed frog caused a decrease in the transcript levels of *Rhbg*, VA and NKA in the dorsal and ventral skin and reduced the capacity of the skin to excrete ammonia (Cruz et al., 2013). Therefore, observations from ammonia-excreting tissues of freshwater animals exhibit a positive correlation between ammonia transporter transcript levels and ammonia excretion rates. The comparatively high levels of *AeAmt1* transcript along with the elevated ammonia levels of the hemolymph, with decreased ammonia efflux at the anal papillae in *AeAmt1* dsRNA-treated larvae suggest that AeAmt1 is an important ammonia transporter for ammonia excretion at the anal papillae of larval *A. aegypti*. Therefore, the results are in agreement with our hypothesis that the anal papillae express the putative ammonia transporters that are involved in ammonia excretion.

Other ammonia-transporting mechanisms in the anal papillae epithelium

Exposing *A. aegypti* larvae to ouabain (an NKA inhibitor) resulted in NH_4^+ fluxes that were less than half of those measured at the anal papillae of control larvae (Fig. 6A). There are at least two possible explanations for the effect of ouabain on ammonia excretion. First, NKA may transport ammonia as NH_4^+, which competes with K^+ or where there are separate binding sites for these two ions (Skou, 1960; Masui et al., 2002; Cruz et al., 2013). There is considerable evidence for this ammonia transport mechanism in a number of animal epithelia, such as crab gills and the antennal gland (see Weihrauch et al., 2004, for review), frog skin (Cruz et al., 2013), fish gills (Mallery, 1983), the epidermis of planaria (Weihrauch et al., 2012b) and potentially larval zebrafish skin (see Shih et al., 2013). Second, as NKA is co-localized with AeAmt1 on the basal side, it can provide a strong voltage gradient to drive NH_4^+ through AeAmt1 from the hemolymph to the cytosol. Either of these two mechanisms could result in decreased ammonia excretion if NKA is inhibited by ouabain.

Application of bafilomycin A (a VA inhibitor) to larval *A. aegypti* resulted in significantly lower NH_4^+ fluxes measured at the anal papillae relative to control larvae (Fig. 6A). VA in the apical membrane of the anal papillae epithelium excretes H^+, which could then be used in ammonia trapping, with NH_3 being supplied via a putative NH_3 transporter, e.g. RhGP. Evidence for this mechanism of ammonia trapping at the apical membrane of epithelia in freshwater exists in a number of animals, such as zebrafish larval skin (Shih et al., 2013), the planarian epidermis (Weihrauch et al., 2012a), frog skin (Cruz et al., 2013) and fish gills (Wilson et al., 1994). The apical localization of VA in the anal papillae suggests that VA contributes to an ammonia-trapping transport mechanism; however, the specific putative ammonia transporter involved remains to be identified. As AeAmt1 localizes to the basal side, an apical transporter participating in an ammonia-trapping mechanism with VA is likely to be one of the AeRh50 proteins. In addition, like NKA, VA likely contributes to a strong, cytosol negative voltage gradient and inhibition of VA may then also affect NH_4^+ entry across the basal membrane through AeAmt1.

Incubation of mosquito larvae with methazolamide, a CA inhibitor, resulted in NH_4^+ efflux at the anal papillae that was significantly reduced compared with controls (Fig. 6A). This result lends further support for an ammonia-trapping mechanism at the anal papillae, whereby cytoplasmic CA, at least in part, supplies VA with H^+ or where an apical membrane-bound CA directly acidifies the boundary layer. CA has been implicated in contributing to acidification of the fish gill boundary layer through the hydration of CO_2, which results in the production of H^+ which can then serve for ammonia trapping (see Wright and Wood, 2009). Apical membrane-bound CA may do this directly in freshwater; however, cytoplasmic CA may also contribute by providing H^+ for VA (Georgalis et al., 2006). Additionally, one may speculate that CO_2, the substrate for CA, enters the papilla syncytium, via one of AeRh50 proteins on the basal side, as RhGPs have also been strongly implied to function as CO_2 channels (Kustu and Inwood, 2006; Perry et al., 2010).

The amiloride-based inhibitor of NHEs HMA did not affect NH_4^+ fluxes at the anal papillae (Fig. 5); hence, we conclude that amiloride-sensitive NHEs are not involved in ammonia transport by

anal papillae. A leucine amino acid residue substitution in the NHE3 of *A. aegypti* renders this exchanger amiloride insensitive (Pullikuth et al., 2006). Application of S3226, a specific inhibitor of NHE3 in mammals (Schwark et al., 1998), to larval mosquitoes resulted in decreased NH_4^+ efflux at the anal papillae (Fig. 6A), suggesting that an NHE, likely NHE3, plays a role in ammonia excretion. The high molecular mass variant of *Aedes* NHE3 is present in the anal papillae (Fig. 6C) and is located on the apical side of the anal papilla epithelium (Fig. 6B). These results suggest that NHE3 may directly transport ammonia out of the cytosol in exchange for a cation (e.g. Na^+), or by exchanging H^+ with cations that may participate in ammonia trapping.

Putative model of ammonia transport by anal papillae and conclusions

The anal papillae of mosquito larvae are important sites for ammonia excretion, similar to the gills of fish and crustaceans, and the skin of planarians, frogs and larval zebrafish. Based on the results of this study, we propose a working model (see Fig. 7) whereby NH_4^+ enters the cytosol of the syncytial epithelium from the hemolymph through the basal membrane-localized AeAmt1 transporter. This is driven by the cytosol negative voltage potential established by the basal membrane-localized NKA, aided by the apical VA. In the cytosol, NH_4^+ could be directly extruded by an apical NHE3 in exchange for a cation (e.g. Na^+) or may dissociate into NH_3 and H^+. The AeRhGPs have not been localized in the anal papillae; however, if located in the basal membrane, an AeRhGP may mediate entry of NH_3 and CO_2 from the hemolymph. NH_3 could be extruded via an apical AeRhGP in conjunction with H^+ transport by an apical VA (NH_3 trapping). The acidification of the boundary layer by VA, and perhaps also by NHE3, is supported by the hydrolysis of CO_2 to yield H^+ through the activity of CA.

Although a number of the mechanisms in our working model are supported solely by pharmacological studies and remain to be confirmed, the identification and localization of AeAmt1 expression, coupled to the reduction in ammonia excretion when AeAmt1 expression is repressed, strongly implicate AeAmt1 in ammonia excretion by anal papillae of mosquito larvae. The direction of NH_4^+ transport by AeAmt1 is consistent with the Mep/Amt transporters of plants, bacteria and yeast, in that NH_4^+ is conveyed into the cytosol. This is the first animal Mep/Amt protein family member to be implicated in ammonia excretion, a vital physiological process for all animals.

Acknowledgements

The authors thank Jean-Paul Paluzzi for advice on dsRNA experiments and Alex R. Quijada-Rodriguez for aiding with gene analysis.

Competing interests

The authors declare no competing or financial interests.

Author contributions

H.C., A.I. and A.D. designed the study with consultation from D.W. and M.P. H.C., L.M. and A.D. executed all experiments with dsRNA knockdown treatments. H.C. and L.M. executed all immunohistochemical staining for AeAmt1 with VA and NKA of anal papillae sections and all western blots of AeAmt1. P.B. and A.I. executed qPCR experiments. A.I. executed all SIET pharmacology experiments. K.F., J.W. and M.P. executed all immmunohistochemical staining for NHE3 of anal papillae sections and western blots of NHE3. D.W. executed gene analysis. H.C. and A.D. wrote the manuscript with editorial support from D.W. and M.P.

Funding

This work was supported by the Natural Sciences and Engineering Research Council of Canada (NSERC) Discovery Grants to A.D. and D.W. and an Ontario Ministry of Research and Innovation Early Researcher Award to A.D.

References

Braun, M. H., Steele, S. L., Ekker, M. and Perry, S. F. (2009). Nitrogen excretion in developing zebrafish (*Danio rerio*): a role for Rh proteins and urea transporters. *Am. J. Physiol. Ren. Physiol.* **296**, F994-F1005.

Burke, R., Barrera, R., Lewis, M., Kluchinsky, T. and Claborn, D. (2010). Septic tanks as larval habitats for the mosquitoes *Aedes aegypti* and *Culex quinquefasciatus* in Playa-Playita, Puerto Rico. *Med. Vet. Entomol.* **24**, 117-123.

Chasiotis, H. and Kelly, S. P. (2008). Occludin immunolocalization and protein expression in goldfish. *J. Exp. Biol.* **211**, 1524-1534.

Clark, T. M. and Bradley, T. J. (1996). Stimulation of Malpighian tubules from larval *Aedes aegypti* by secretagogues. *J. Insect Physiol.* **42**, 593-602.

Cruz, M. J., Sourial, M. M., Treberg, J. R., Fehsenfeld, S., Adlimoghaddam, A. and Weihrauch, D. (2013). Cutaneous nitrogen excretion in the African clawed frog *Xenopus laevis*: effects of high environmental ammonia (HEA). *Aquat. Toxicol.* **136-137**, 1-12.

Del Duca, O., Nasirian, A., Galperin, V. and Donini, A. (2011). Pharmacological characterisation of apical Na+ and Cl– transport mechanisms of the anal papillae in the larval mosquito *Aedes aegypti*. *J. Exp. Biol.* **214**, 3992-3999.

Donini, A. and O'Donnell, M. J. (2005). Analysis of Na^+, Cl^-, K^+, H^+ and NH_4^+ concentration gradients adjacent to the surface of anal papillae of the mosquito Aedes aegypti: application of self-referencing ion-selective microelectrodes. *J. Exp. Biol.* **208**, 603-610.

Edwards, H. A. and Harrison, J. B. (1983). An osmoregulatory syncytium and associated cells in a freshwater mosquito. *Tissue Cell* **15**, 271-280.

Furriel, R. P. M., Masui, D. C., McNamara, J. C. and Leone, F. A. (2004). Modulation of gill Na^+,K^+-ATPase activity by ammonium ions: putative coupling of nitrogen excretion and ion uptake in the freshwater shrimp Macrobrachium olfersii. *J. Exp. Zool.* **301A**, 63-74.

García Romeu, F. and Salibián, A. (1968). Sodium uptake and ammonia excretion through the skin of the South American frog (L., 1758). *Life Sci.* **7**, 465-470.

Georgalis, T., Gilmour, K. M., Yorston, J. and Perry, S. F. (2006). Roles of cytosolic and membrane-bound carbonic anhydrase in renal control of acid-base balance in rainbow trout, Oncorhynchus mykiss. *Am. J. Physiol. Ren. Phys.* **291**, F407-F421.

Gruswitz, F., Chaudhary, S., Ho, J. D., Schlessinger, A., Pezeshki, B., Ho, C.-M., Sali, A., Westhoff, C. M. and Stroud, R. M. (2010). Function of human Rh based on structure of RhCG at 2.1 Å. *Proc. Nat. Acad. Sci. USA* **107**, 9638-9643.

Gu, R., Duan, F., An, X., Zhang, F., von Wiren, N. and Yuan, L. (2013). Characterization of AMT-mediated high-affinity ammonium uptake in roots of maize (Zea mays L.). *Plant Cell Physiol.* **54**, 1515-1524.

Ip, Y. K., Loong, A. M., Kuah, J. S., Sim, E. W. L., Chen, X. L., Wong, L. P., Lam, S. H., Delgado, I. L. S., Wilson, J. M. and Chew, S. F. (2012). Roles of three branchial Na^+ - K^+ - ATPase α-subunit isoforms in freshwater adaptation, seawater acclimation, and active ammonia excretion in Anabas testudineas. *Am. J. Physiol.* **303**, R112-R125.

Jonusaite, S., Kelly, S. P. and Donini, A. (2011). The physiological response of larval Chironomus riparius (Meigen) to abrupt brackish water exposure. *J. Comp. Physiol. B* **181**, 343-352.

Khademi, S., O'Connell, J., III, Remis, J., Robles-Colmenares, Y., Miercke, L. J. W. and Stroud, R. M. (2004). Mechanism of ammonia transport by Amt/MEP/Rh: Structure of AmtB at 1.35 Å. *Science* **305**, 1587-1594.

Kustu, S. and Inwood, W. (2006). Biological gas channels for NH3 and CO2: evidence that Rh (Rhesus) proteins are CO2 channels. *Transfus. Clin. Biol.* **13**, 103-110.

MacVicker, J. A., Billingsley, P. F. and Djamgoz, M. B. (1993). ATPase activity in the midgut of the mosquito, Anopheles stephensi: biochemical characterization of ouabain-sensitive and ouabain-insensitive activities. *J. Exp. Biol.* **174**, 167-183.

Mallery, C. H. (1983). A carrier enzyme basis for ammonium excretion in teleost gill. NH_4^+-stimulated Na-dependent ATPase activity in Opsanus beta. *Comp. Biochem. Physiol. A Physiol.* **74**, 889-897.

Marcaggi, P., Thwaites, D. T., Deitmer, J. W. and Coles, J. A. (1999). Chloride-dependent transport of NH4+ into bee retinal glial cells. *Eur. J. Neurosci.* **11**, 167-177.

Masui, D. C., Furriel, R. P. M., McNamara, J. C., Mantelatto, F. L. M. and Leone, F. A. (2002). Modulation by ammonium ions of gill microsomal (Na^+, K^+)-ATPase in the swimming crab Callinectes danae: a possible mechanism for regulation of ammonia excretion. *Comp. Biochem. Physiol. C Toxicol. Pharmacol.* **132**, 471-482.

Mullins, D. E. (1974). Nitrogen metabolism in the American cockroach: an examination of whole body ammonium and other cations excreted in relation to water requirements. *J. Exp. Biol.* **61**, 541-556.

Nakhoul, N. L. and Hamm, L. L. (2014). The challenge of determining the role of Rh glycoproteins in transport of NH3 and NH4+. *Wiley Interdiscip. Rev. Membr. Transp. Signal.* **3**, 53-61.

Nawata, C. M., Hung, C. C. Y., Tsui, T. K. N., Wilson, J. M., Wright, P. A. and Wood, C. M. (2007). Ammonia excretion in rainbow trout (Oncorhynchus mykiss): evidence for Rh glycoprotein and H+-ATPase involvement. *Physiol. Genomics* **31**, 463-474.

Nawata, C. M., Wood, C. M. and O'Donnell, M. J. (2010). Functional characterization of Rhesus glycoproteins from an ammoniotelic teleost, the

rainbow trout, using oocyte expression and SIET analysis. *J. Exp. Biol.* **213**, 1049-1059.
Nguyen, H. and Donini, A. (2010). Larvae of the midge Chironomus riparius possess two distinct mechanisms for ionoregulation in response to ion-poor conditions. *Am. J. Physiol. Regul. Integr. Comp. Physiol.* **299**, R762-R773.
Nygaard, T. P., Rovira, C., Peters, G. H. and Jensen, M. O. (2006). Ammonium recruitment and ammonia transport by E. coli ammonia channel AmtB. *Biophys. J.* **91**, 4401-4412.
Orlowski, J. and Grinstein, S. (2004). Diversity of the mammalian sodium/proton exchanger SLC9 gene family. *Pflügers Arch.* **447**, 549-565.
Patrick, M. L., Aimanova, K., Sanders, H. R. and Gill, S. S. (2006). P-type Na^+/K^+-ATPase and V-type H+-ATPase expression patterns in the osmoregulatory organs of larval and adult mosquito Aedes aegypti. *J. Exp. Biol.* **209**, 4638-4651.
Peng, J. and Huang, C. H. (2006). Rh proteins versus Amt proteins: an organismal and phylogenetic perspective on CO2 and NH3 gas channels. *Transfus. Clin. Biol.* **13**, 85-94.
Perry, S. F., Braun, M. H., Noland, M., Dawdy, J. and Walsh, P. J. (2010). Do zebrafish Rh proteins act as dual ammonia-CO2 channels? *J. Exp. Zool. A Ecol. Genet. Physiol.* **313A**, 618-621.
Pfaffl, M. W. (2004). Real-time RT-PCR: new approaches for precise mRNA quantification. *Biospek* **10**, 92-95.
Pitts, R. J., Derryberry, S. L., Jr., Pulous, F. E. and Zweibel, L. J. (2014). Antennal-expressed ammonium transporters in the malaria vector mosquito Anopheles gambiae. *PLoS ONE* **9**, e111858.
Pullikuth, A., Aimanova, K., Kang'ethe, W., Sanders, H. R. and Gill, S. S. (2006). Molecular characterization of sodium/proton exchanger 3 (NHE3) from the yellow fever vector, Aedes aegypti. *J. Exp. Biol.* **209**, 3529-3544.
Ramasamy, R. and Surendran, S. N. (2012). Global climate change and its potential impact on disease transmission by salinity-tolerant mosquito vectors in coastal zones. *Front. Physiol.* **3**, 198.
Schwark, J.-R., Jansen, H. W., Lang, H.-J., Krick, W., Burckhardt, G. and Hropot, M. (1998). S3226, a novel inhibitor of Na+/H+ exchanger subtype 3 in various cell types. *Pflugers Arch.* **436**, 797-800.
Shih, T.-H., Horng, J.-L., Hwang, P.-P. and Lin, L.-Y. (2008). Ammonia excretion by the skin of zebrafish (Danio rerio) larvae. *Am. J. Physiol. Cell Physiol.* **295**, C1625-C1632.
Shih, T.-H., Horng, J.-L., Lai, Y.-T. and Lin, L.-Y. (2013). Rhcg1 and Rhbg mediate ammonia excretion by ionocytes and keratinocytes in the skin of zebrafish larvae: H+-ATPase-linked active ammonia excretion by ionocytes. *Am. J. Physiol. Regul. Integr. Comp. Physiol.* **304**, R1130-R1138.
Singh, A. D., Wong, S., Ryan, C. P. and Whyard, S. (2013). Oral delivery of double-stranded RNA in larvae of the yellow fever mosquito, Aedes aegypti: implications for pest mosquito control. *J. Insect Sci.* **13**, 1-18.
Skou, J. C. (1960). Further investigations on a Mg+++Na+-activated adenosintriphosphatase, possibly related to the active, linked transport of Na+ and K+ across the nerve membrane. *Biochim. Biophys. Acta* **42**, 6-23.
Sohal, R. S. and Copeland, E. (1966). Ultrastructural variations in the anal papillae of Aedes aegypti (L.) at different environmental salinities. *J. Insect Physiol.* **12**, 429-434.
Soupene, E., Inwood, W. and Kustu, S. (2004). Lack of the Rhesus protein Rh1 impairs growth of the green alga Chlamydomonas reinhardtii at high CO2. *Proc. Natl. Acad. Sci. USA* **101**, 7787-7792.
Thomson, R. B., Thomson, J. M. and Phillips, J. E. (1988). NH4+ transport in acid-secreting insect epithelium. *Am. J. Physiol.* **254**, R348-R356.
Thornton, J., Blakey, D., Scanlon, E. and Merrick, M. (2006). The ammonia channel protein AmtB from Escherichia coli is a polytopic membrane protein with a cleavable signal peptide. *FEMS Microbiol. Lett.* **258**, 114-120.
Tsui, T. K. N., Hung, C. Y. C., Nawata, C. M., Wilson, J. M., Wright, P. A. and Wood, C. M. (2009). Ammonia transport in cultured gill epithelium of freshwater rainbow trout: the importance of Rhesus glycoproteins and the presence of an apical Na+/NH4+ exchange complex. *J. Exp. Biol.* **212**, 878-892.
Vallon, V., Schwark, J. R., Richter, K. and Hropot, M. (2000). Role of Na+/H+ exchanger NHE3 in nephron function: Micropuncture studies with S3226, an inhibitor of NHE3. *Am. J. Physiol.* **278**, F375-F379.
Weihrauch, D. (2006). Active ammonia absorption in the midgut of the Tobacco hornworm Manduca sexta L.: transport studies and mRNA expression analysis of a Rhesus-like ammonia transporter. *Insect Biochem. Mol. Biol.* **36**, 808-821.
Weihrauch, D., Morris, S. and Towle, D. W. (2004). Ammonia excretion in aquatic and terrestrial crabs. *J. Exp. Biol.* **207**, 4491-4504.
Weihrauch, D., Wilkie, M. P. and Walsh, P. J. (2009). Ammonia and urea transporters in gills of fish and aquatic crustaceans. *J. Exp. Biol.* **212**, 1716-1730.
Weihrauch, D., Chan, A. C., Meyer, H., Doring, C., Sourial, M. O'Donnell, M. J. (2012a). Ammonia excretion in the freshwater planarian Schmidtea mediterranea. *J. Exp. Biol.* **215**, 3242-3253.
Weihrauch, D., Donini, A. and O'Donnell, M. J. (2012b). Ammonia transport by terrestrial and aquatic insects. *J. Insect Physiol.* **58**, 473-487.
Willmann, A., Weiß, M. and Nehls, U. (2007). Ectomycorrhiza-mediated repression of the high-affinity ammonium importer gene AmAMT2 in Amanita muscaria. *Curr. Genet.* **51**, 71-78.
Wilson, R., Wright, P., Munger, S. and Wood, C. M. (1994). Ammonia excretion in freshwater Rainbowtrout (Oncorhynchus mykiss) and the importance of gill boundary layer acidification: lack of evidence for Na+/NH4+exchange. *J. Exp. Biol.* **191**, 37-58.
Wright, P. A. and Wood, C. M. (2009). A new paradigm for ammonia excretion in aquatic animals: role of Rhesus (Rh) glycoproteins. *J. Exp. Biol.* **212**, 2303-2312.
Wu, X., Yan, H., Qu, C., Xu, Z., Li, W., Hao, B., Yang, C., Sun, G. and Liu, G. (2015). Sequence and expression analysis of the AMT gene family in poplar. *Front. Plant Sci.* **6**, 337.
Yuan, L., Graff, L., Loque, D., Kojima, S., Tsuchiya, Y. N., Takahashi, H. and von Wiren, N. (2009). AtAMT1;4, a pollen-specific high-affinity ammonium transporter of the plasma membrane in Arabidopsis. *Plant Cell Physiol.* **50**, 13-25.
Zachos, N. C., Tse, M. and Donowitz, M. (2005). Molecular physiology of intestinal N+/H+ exchange. *Ann. Rev. Physiol.* **67**, 411-443.